

Order and Disorder in AKLT Antiferromagnets in Three Dimensions

Siddharth A. Parameswaran,^{1,*} S. L. Sondhi,^{1,2,†} and Daniel P. Arovas^{3,‡}

¹*Department of Physics, Joseph Henry Laboratories,
Princeton University, Princeton, New Jersey 08544, USA*

²*Princeton Center for Theoretical Science, Princeton University, Princeton, New Jersey 08544, USA*

³*Department of Physics, University of California at San Diego, La Jolla, California 92093, USA*

(Dated: July 21, 2008)

The models constructed by Affleck, Kennedy, Lieb, and Tasaki¹ describe a family of quantum antiferromagnets on arbitrary lattices, where the local spin S is an integer multiple M of half the lattice coordination number. The equal time quantum correlations in their ground states may be computed as finite temperature correlations of a classical $O(3)$ model on the same lattice, where the temperature is given by $T = 1/M$. In dimensions $d = 1$ and $d = 2$ this mapping implies that all AKLT states are quantum disordered. We consider AKLT states in $d = 3$ where the nature of the AKLT states is now a question of detail depending upon the choice of lattice and spin; for sufficiently large S some form of Néel order is almost inevitable. On the unfrustrated cubic lattice, we find that all AKLT states are ordered while for the unfrustrated diamond lattice the minimal $S = 2$ state is disordered while all other states are ordered. On the frustrated pyrochlore lattice, we find (conservatively) that several states starting with the minimal $S = 3$ state are disordered. The disordered AKLT models we report here are a significant addition to the catalog of magnetic Hamiltonians in $d = 3$ with ground states known to lack order on account of strong quantum fluctuations.

I. INTRODUCTION

Quantum antiferromagnets have been a fertile field of research for a half century, exhibiting a great richness and variety of physical phenomena. In more recent decades, starting with Anderson's introduction of the RVB state² and accelerating with the discovery of the cuprate superconductors³, much attention has focused on antiferromagnets that allow for disordered ground states due to a mix of frustration and quantum fluctuations⁴. In an important step, Affleck *et. al*¹ showed how to construct models that build in a great deal of both these effects by using local projectors - models for which (essentially unique) ground states can be determined analytically. These AKLT models have spins given by $S = \frac{z}{2}M$, where M is any integer, and z the lattice coordination number. The associated ground states have the added feature that their wavefunctions can be written in Jastrow (pair product) form. A general feature of such wavefunctions is that the ground-state probability densities can be viewed as Boltzmann weights corresponding to a local, indeed nearest neighbor, Hamiltonian for classical spins on the same lattice. Using this unusual quantum-classical equivalence we can understand many properties of the states via Monte Carlo simulations of the associated classical model.

In $d = 1$ and $d = 2$, the AKLT states are disordered for *any* spin due to the Hohenberg-Mermin-Wagner theorem. In particular, the $d = 1$ case is the celebrated AKLT chain which realizes the $S = 1$ Haldane phase. In this paper, we study AKLT states in $d = 3$, which are relatively less well-understood than their one and two dimensional counterparts. Moreover, in three dimensions, the Hohenberg-Mermin-Wagner theorem no longer applies and therefore whether an AKLT state of a given spin

is disordered or instead exhibits long range order is no longer automatic. Instead a computation is now required to settle this question and it is this issue that we address in this paper by a combination of mean-field arguments and Monte Carlo simulation. Specifically, we discuss the AKLT states on the simple cubic and diamond lattices, where there is no (geometrical) frustration, as well on the highly frustrated pyrochlore lattice, where the attendant complications lead to a macroscopic ground state degeneracy of the associated classical model. Of course, all the models we study have frustration from competing interactions.

On the cubic lattice we find that all AKLT states starting with the "minimal" (smallest spin) $S = 3$ state are ordered with the standard two sublattice Néel pattern. The diamond lattice has a small coordination number and thus larger fluctuations and we find that on it the minimal $S = 2$ state is disordered while all higher spin states are ordered with the two sublattice Néel pattern. On the pyrochlore lattice, the geometrical frustration of the lattice plays a significant role. In mean field theory for the companion classical model we find a macroscopic number of solutions corresponding to as many energy minima. While the mean field estimate for the critical spin (transition temperature) already indicates that the minimal $S = 3$ model on the pyrochlore lattice is disordered, the large number of competing states indicate that the true boundary between disorder and some form of order lies at much larger values of spin. Indeed, a basic simulation leads to a conservative bound in which disordered ground states persist up to $S = 15$. Given the unphysical complexity of the AKLT Hamiltonians at such large spins we do not pursue a more precise determination of this boundary in this work. Indeed, readers may take as the main fruits of our work the identifica-

tion of the $S = 2$ AKLT model on the diamond lattice and the $S = 3$ AKLT model on the pyrochlore lattice as (not too common) instances of three dimensional spin Hamiltonians with quantum disordered ground states.

It is worth noting that models with quantum disordered ground states are currently objects of intense interest in the context of topological order and more specifically, in the context of topological quantum computing. We note that our disordered models do *not* yield topologically ordered states; they do not possess a topological degeneracy or host fractionalized excitations. The disordered states herein are described either as fully symmetric valence bond solids or, in the long wavelength sense, as quantum paramagnets. To understand why this is the case, it is instructive to recall how a closely related strategy works to produce topologically ordered states in $S = 1/2$ models, including instances in $d = 3$. This strategy, initiated by Chayes, Chayes and Kivelson⁵, and brought to fruition in work by Raman, Moessner and Sondhi⁶ works with spin- $\frac{1}{2}$ analogs of the AKLT models called Klein models⁷. Unlike AKLT models, Klein models have many ground states—indeed they select the macroscopically many nearest neighbor valence bond coverings of a lattice. This selection of a degenerate manifold underlies the emergence of topological order. More precisely, the work of RMS showed that Klein models could be controllably perturbed on a family of lattices in order to select a topologically ordered (RVB) state in this ground state manifold. In this fashion they could construct SU(2) symmetric models with Z_2 topological order in $d = 2$ but also models with Z_2 and U(1) order in $d = 3$ ⁸.

The rest of this paper is organized as follows: In Section II, we present a brief summary of the AKLT construction. We then proceed in Section III to review the mean field analysis of the AKLT states⁹. We then specialize in Section IV to bipartite lattices, and compute the transition temperature for the simple cubic and diamond lattices using Monte Carlo simulations. We determine that while the simple cubic lattice exhibits Néel order for all choices of M (and thus S), the diamond lattice allows a quantum disordered state in the $M = 1$ ($S = 2$) case. We then go on to discuss the AKLT states on the frustrated 3D pyrochlore lattice, and discuss the mean field analysis and classical ground states in this case. We find that the pyrochlore lattice admits quantum disordered states for many values of M ; while the exact value of M_c was not determined, we find evidence from simulations that it exceeds 5, corresponding to $S = 15$.

II. AKLT STATES: A BRIEF REVIEW

The central idea of the AKLT approach¹, is to use the idea of quantum singlets to construct correlated quantum-disordered wavefunctions, which are eigenstates of local projection operators. One can then produce many-body Hamiltonians using projectors that ex-

tinguish the state, thereby rendering the parent wavefunction an exact ground state, typically with a gap to low-lying excitations. A general member of the family of valence bond solid (AKLT) states can be written compactly in terms of Schwinger bosons¹⁰:

$$|\Psi(\mathcal{L}; M)\rangle = \prod_{\langle ij \rangle} \left(b_{i\uparrow}^\dagger b_{j\downarrow}^\dagger - b_{i\downarrow}^\dagger b_{j\uparrow}^\dagger \right)^M |0\rangle. \quad (1)$$

This assigns M singlet creation operators to each link $\langle ij \rangle$ of a lattice \mathcal{L} . The total boson occupancy per site is given by zM , where z is the lattice coordination number, and the resultant spin on each site is given by $S = \frac{1}{2}zM$. Thus, given any lattice, the above construction defines a family of AKLT states with $S = \frac{1}{2}zM$, where M is any integer. The maximum possible spin on any link is then $S_{ij}^{\max} = 2S - M$, and therefore $|\Psi(\mathcal{L}; M)\rangle$ is extinguished by any Hamiltonian constructed out of projectors $P_J(ij)$ onto link spin J , provided $2S - M + 1 \leq J \leq 2S$. The projectors, which transform as SU(2) singlets, may be written as polynomials in the Heisenberg coupling $\vec{S}_i \cdot \vec{S}_j$ of order $2S$. Explicitly, one has

$$P_J(ij) = \prod_{\substack{J'=0 \\ (J' \neq J)}}^{2S} \frac{\vec{S}_i \cdot \vec{S}_j + S(S+1) - \frac{1}{2}J'(J'+1)}{\frac{1}{2}J(J+1) - \frac{1}{2}J'(J'+1)}. \quad (2)$$

The AKLT states have a convenient representation in terms of SU(2) coherent states, as first shown in Ref. 10. In terms of the Schwinger bosons, the normalized spin- S coherent state is given by $|\hat{n}\rangle = (p!)^{-1/2} (z_\mu b_\mu^\dagger)^p |0\rangle$, where $p = 2S$, with $z = (u, v)$ a CP^1 spinor, with $u = \cos(\theta/2)$ and $v = \sin(\theta/2) e^{i\varphi}$. The unit vector \hat{n} is given by $n^a = z^\dagger \sigma^a z$, where σ are the Pauli matrices. In the coherent state representation, the general AKLT state wavefunction is the pair product $\Psi = \prod_{\langle ij \rangle} (u_i v_j - v_i u_j)^M$. Following Ref. 10, we may write $|\Psi|^2 \equiv \exp(-H_{\text{cl}}/T)$ as the Boltzmann weight for a classical O(3) model with Hamiltonian

$$H_{\text{cl}} = - \sum_{\langle ij \rangle} \ln \left(\frac{1 - \hat{n}_i \cdot \hat{n}_j}{2} \right), \quad (3)$$

at temperature $T = 1/M$. All equal time quantum correlations in the state $|\Psi\rangle$ may then be expressed as classical, finite temperature correlations of the Hamiltonian H_{cl} .

The consequences of this quantum-to-classical equivalence, which is a general feature of Jastrow (pair product) wavefunctions, were noted in Ref. 10. On one and two-dimensional lattices, the Hohenberg-Mermin-Wagner theorem precludes long-ranged order at any finite value of the discrete quantum parameter M . Thus, while the $S = 2$ Heisenberg model on the square lattice is rigorously known to have a Néel ordered ground state¹¹, the $S = 2$ AKLT Hamiltonian, which includes up to biquartic terms, has a featureless quantum disordered ground state, called a ‘quantum paramagnet’. In three dimensions, we expect Néel order for large M , corresponding

to low temperatures in the classical model. If the Néel temperature for H_{cl} on a given lattice satisfies $T_c > 1$, then $M_c < 1$, and all the allowed AKLT states on that lattice exhibit long-ranged order.

The issue of whether or not the AKLT states can be in the quantum disordered phase on a given lattice can be investigated by a combination of mean-field calculations and classical Monte Carlo simulations, which we present below.

III. MEAN FIELD THEORY

A mean field analysis of the classical model of eqn. 3 on bipartite lattices was described in Refs. 9,10. In the general case, we may begin with the Hamiltonian of eqn. 3, and we write $\hat{n}_i = \vec{m}_i + \delta\hat{n}_i$, with $\langle \hat{n}_i \rangle = \vec{m}_i$. Expanding H_{cl} to order $\delta\hat{n}_i$, we obtain the mean field Hamiltonian $\tilde{H}^{\text{MF}} = E_0 - \sum_i \vec{h}_i \cdot \hat{n}_i$, where the mean field \vec{h}_i is given by

$$\vec{h}_i = - \sum_j' \frac{\vec{m}_j}{1 - \vec{m}_i \cdot \vec{m}_j}, \quad (4)$$

where the prime restricts the sum on j to nearest neighbors of site i . Self-consistency then requires

$$\vec{m}_i = \langle \hat{n}_i \rangle = \frac{\int d\hat{n}_i \hat{n}_i \exp(\vec{h}_i \cdot \hat{n}_i/T)}{\int d\hat{n}_i \exp(\vec{h}_i \cdot \hat{n}_i/T)}, \quad (5)$$

which yields $\vec{m}_i = m_i \vec{h}_i/|\vec{h}_i|$, with local magnetization

$$m_i = \coth\left(\frac{h_i}{T}\right) - \frac{T}{h_i}. \quad (6)$$

IV. UNFRUSTRATED LATTICES: SIMPLE CUBIC AND DIAMOND

A. Mean Field Transition

On an unfrustrated, bipartite, lattice a sublattice rotation $\hat{n}_i \rightarrow \eta_i \hat{n}_i$, with $\eta_i = \pm 1$ on the A (B) sublattice, results in a ferromagnetic interaction, and if we posit a uniform local magnetization \vec{m} we obtain the mean field

$$h = \frac{z m}{1 + m^2}, \quad (7)$$

where z is the lattice coordination number. This results in a mean field transition temperature $T_c^{\text{MF}} = \frac{1}{3}z$, *i.e.* $M_c^{\text{MF}} = 3z^{-1}$. All AKLT states on bipartite lattices in more than two space dimensions will exhibit two sublattice Néel order, provided $M > M_c$. According to the mean field analysis, long ranged order should pertain for $z \geq 3$, which would be satisfied by almost any three-dimensional structure. However, mean field theory

ignores fluctuations, hence it overestimates T_c and underestimates M_c . Therefore the possibility remains that a quantum disordered AKLT state may exist in a three-dimensional lattice. We examine two cases, the simple cubic lattice ($z = 6$) and the diamond lattice ($z = 4$). We shall address this issue via classical Monte Carlo simulations of our model on both lattices. We note that, of these, the diamond lattice is the stronger candidate as it is more weakly coordinated, and $M_c^{\text{MF}} = \frac{3}{4}$ is sufficiently close to threshold that fluctuations are likely to drive the true M_c to be greater than unity.

B. Monte-Carlo Simulations

The classical Hamiltonian H_{cl} of eqn. 3 consists of nearest neighbor interactions $v(\vartheta_{ij})$ where $\vartheta_{ij} = \cos^{-1}(\hat{n}_i \cdot \hat{n}_j)$ is the relative angle between spins on neighboring sites i and j , and $v(\vartheta) = -\ln \sin^2(\frac{1}{2}\vartheta)$. This interaction strongly suppresses ferromagnetic alignment, with a logarithmically infinite barrier, but has a smooth quadratic minimum $v(\vartheta) \approx \frac{1}{4}(\vartheta - \pi)^2$ when $\vartheta \approx \pi$. We have simulated the equivalent ferromagnetic model, with interaction $v(\vartheta) = -\ln \cos^2(\frac{1}{2}\vartheta)$.

We used a multithread Monte Carlo approach, in which simultaneous simulations with independent initial configurations were used to produce M independent Markov chains each with N configurations¹², which were then written to a file. For every independent thread, we performed checkerboard sweeps of the lattice using a standard Metropolis Monte Carlo technique¹³. In each Monte Carlo step, we produced a vector $\delta\hat{n}$, with length distributed according to a Gaussian and pointing in a random direction, which was used to generate a new spin unit vector

$$\hat{n}'_i = \frac{\hat{n}_i + \delta\hat{n}}{|\hat{n}_i + \delta\hat{n}|} \quad (8)$$

The standard deviation of the Gaussian was adjusted by hand until a significant fraction of proposed moves were accepted (we left it at $\sigma = 0.5$.)

The number of Monte Carlo steps per site (MCS) and the number of independent threads were adjusted to count roughly the same number of autocorrelation times for each sample size¹⁴. For each chain, we obtained the average value of the Binder cumulant, and averaged this across chains to get a single number for each temperature. We estimated the error from the standard deviation of the M independent thread averages. This is free of the usual complications of correlated samples inherent in estimating the error from a single chain, and frees us of the need to compute autocorrelation times to weight our error estimate.

Plots were made of the Binder cumulant¹⁵, defined to be

$$B = 1 - \frac{\langle (\vec{M}^2)^2 \rangle}{3 \langle \vec{M}^2 \rangle^2}, \quad (9)$$

where $\vec{M} = \sum_i \hat{n}_i$ is the total magnetization.

For any system of Heisenberg spins in the thermodynamic limit, the Binder cumulant has value $\frac{2}{3}$ in the low-temperature (ordered) phase and value $\frac{4}{9}$ in the high-temperature phase. These are easily seen by assuming a gaussian distribution for $|\vec{M}|$ at high temperature, and using the result that all the expectation values of powers of $\vec{M} \cdot \vec{M}$ are equal in the ordered phase. For a finite system, the limiting values continue to be close to these estimates, but the interpolating behavior is different for each system size; the primary utility from our point of view is that finite-size scaling analysis of B reveals that it has a fixed point at the transition temperature¹⁵. We may therefore determine T_c by plotting the Binder cumulant for a series of different lattice sizes, and determining the points where the curves cross.

Before simulating our modified interaction, we checked our code by determining the (known) transition temperatures for the standard Heisenberg model on the simple cubic lattice¹³ and the Ising model on both the diamond and the simple cubic lattices¹⁶, as well as comparing the high-temperature susceptibility from simulations to the predictions of the high-temperature expansion¹⁷. All these agreed well with the expected values, at least to the accuracy we need to determine whether T_c is less than or greater than 1. Recall that if $T_c < 1$, then $M_c > 1$, which means that the minimal AKLT state, with $M = 1$, is on the disordered side of the phase transition.

Using our Monte Carlo simulations, we obtain estimates of T_c for the families of AKLT states on the simple cubic and diamond lattices. Although our simulation techniques were not particularly sophisticated, they were sufficient to pin down T_c to a reasonable degree of accuracy, and certainly enough to determine whether $T_c > 1$. Our simulations allow us to estimate that $T_c^{\text{SC}} \approx 1.66$ on the simple cubic lattice, and that $T_c^{\text{D}} \approx 0.85$ for the diamond structure. Therefore, we conclude that while all the simple cubic AKLT states are Néel-ordered, the minimal ($S = 2$) AKLT state in diamond is a featureless quantum disordered state.

V. FRUSTRATED LATTICE: THE PYROCHLORE

The pyrochlore is a lattice of corner-sharing tetrahedra and can be constructed from the the diamond lattice by placing a site at the midpoint of each bond, resulting in a quadripartite structure. The pyrochlore lattice is highly frustrated from the perspective of of collinear antiferromagnetism; the canonical nearest-neighbor classical Heisenberg antiferromagnet on this lattice has an extensive ground-state degeneracy and remains a quantum paramagnet at all temperatures¹⁸.

Our problem has a different form for the interaction and hence the results for the nearest neighbor problem, which build on the high degree of degeneracy for a single tetrahedron, do not apply. Indeed, as we discuss below,

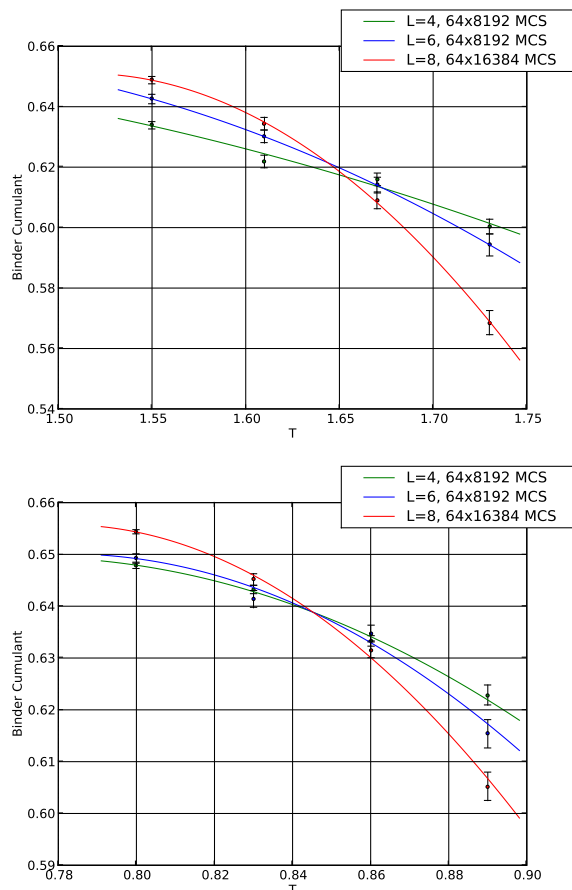


FIG. 1: Binder cumulant plots for the valence-bond states on the cubic and diamond lattices. The T -axis scale is chosen using a rough estimate of T_c so as to provide approximately the same window in natural units T/T_c for both cases. In each case, the total number of spins being simulated is $2 \cdot L^3$. We perform a fit of the data (weighted by the error bars) to a parabola and estimate T_c from the intersection of the best-fit lines. We can be reasonably confident that the curves have an intersection from the fact that they change order on either side of the crossing, and become separated by more than a standard deviation as we move away from the crossing. We obtain $T_c \approx 1.66$ for the cubic lattice and $T_c \approx 0.85$ for diamond.

the logarithmic form of the interaction energy leads to the selection of a unique single-tetrahedron ground state up to global rotations. However, the full lattice still exhibits a substantial ground state degeneracy on account of its open architecture indicating an anomalously low transition temperature which we roughly bound from above by $T \approx 0.2$. We now turn to the details of these assertions.

A. Single-Tetrahedron Ground States

Numerical minimization on a single tetrahedron finds the lowest-energy configuration to be one where each pair

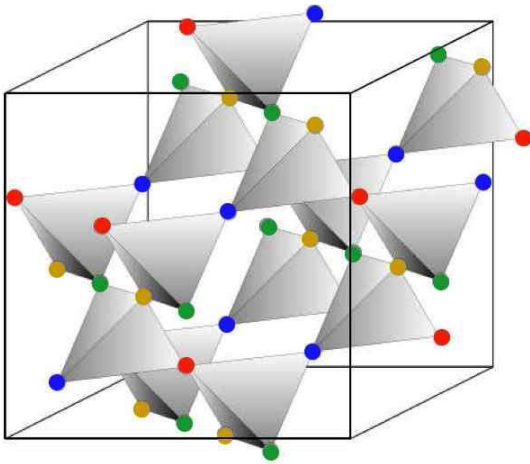


FIG. 2: The quadripartite pyrochlore lattice, which is formed out of corner-sharing tetrahedra.

of spins make an angle $\vartheta_{ij} = \cos^{-1}(\hat{n}_i \cdot \hat{n}_j) = \cos^{-1}(-\frac{1}{3})$. This means that the spins are pointing either towards or away from the corners of a regular tetrahedron in three-dimensional spin space. We proceed to search for soft modes, by expanding the energy to quadratic order and studying the resulting normal modes. We find that there is a pair of soft modes corresponding to global rotations, and another where three spins rotate about the axis defined by the fourth. The latter mode leads to a degeneracy of ground states of the full lattice as discussed below.

We note that for the Heisenberg antiferromagnet with interaction $\hat{n}_i \cdot \hat{n}_j$, the single tetrahedron Hamiltonian is $H_\Gamma = (\vec{M}_\Gamma)^2$, where $\vec{M}_\Gamma = \sum_{i \in \Gamma} \hat{n}_i$ is a sum of the spin vectors over all sites in the tetrahedron Γ . The ground state manifold $\vec{M}_\Gamma = 0$ is then five-dimensional, since one can choose any two vectors \hat{n}_A and \hat{n}_B , then take $\hat{n}_C = -\hat{n}_A$ and $\hat{n}_D = -\hat{n}_B$. The four freedoms associated with choosing \hat{n}_A and \hat{n}_B are then augmented by another freedom to rotate the C and D spins about the direction $\hat{n}_A + \hat{n}_B$. A large- N analysis¹⁹ finds that the $O(N)$ pyrochlore antiferromagnet is paramagnetic down to $T = 0$.

B. Ground States on the Full Lattice

There are many ways in which we can construct degenerate states on the lattice that simultaneously satisfy the minimum-energy constraint on every tetrahedron. We begin by describing the simplest such states which form a discrete family. To this end, label the four spins defined by the single-tetrahedron constraint (with a fixed joint orientation) as A , B , C and D . If we use only these four orientations for each spin, we have the constraint that none of them can occur twice on the same tetrahedron; this translates to the statement that spins on neighboring links must be different. This is the same constraint as for ground states of the antiferromagnetic 4-

state Potts model. We therefore conclude that one family of ground states of the classical Hamiltonian on the pyrochlore lattice are in a one-to-one correspondence with the ground states of the 4-state Potts antiferromagnet on the pyrochlore lattice. Readers familiar with the lore on the kagomé problem²⁰ will recognize the resemblance to the planar ground states there which are in correspondence to ground states of the 3-state Potts model. As in the kagomé problem, from this set of ground states others can be constructed by identifying sets of spins which can be locally rotated by an arbitrary amount at zero energy cost. These are sets of spins, say of type B , C and D which are connected to other spins solely by spins of type A . Clearly one can rotate this set by an angle about the A axis at zero energy cost.

While we have not parametrized the full, continuous, space of ground states an extensive lower bound on the degeneracy of the ‘Potts submanifold’ of ground states can be obtained as follows. First, we note that the number of allowed configurations of the 3-state Potts model on a kagomé lattice with M sites is given^{20,21} by $g_k \approx (1.20872)^{(2M/3)}$. Next we partition the pyrochlore into four sublattices, so that the sites that lie on a single tetrahedron are each on different sublattices. Choose one sublattice, and fix the spins on that sublattice to be one of the four types (say A .) Now, looking down through the tetrahedra, one sees alternating layers of triangular and kagomé planes; the kagomé planes are made up of B , C , and D spins, while the triangular planes are made up of A spins. In each kagomé plane, we have M spins, whose configurations are those of the 3-state Potts model. If we now let N_k be the number of kagomé planes, we must have that $M \cdot N_k = \frac{3}{4}N$, where N is the total number of spins in the system. We then have for the number of states in this restricted submanifold

$$g_{\text{restricted}} = 4 \cdot g_k^{N_k} \approx 4 \cdot (1.20872)^{N/2} \quad (10)$$

where the factor of 4 stems from the fact that we can choose any one of the four spins to be fixed in the triangular planes. Since we’ve restricted ourselves to considering a certain submanifold of the ground states in the above argument, it is clear that we have obtained a lower bound for the degeneracy of the Potts submanifold.

C. Bounds on T_c

Each of the ground states identified above can serve as a basis for a mean-field treatment of the system and all of them yield the same T_c^{MF} . This vast set of ‘‘soft modes’’ is, of course, a signature that the true $T_c \ll T_c^{\text{MF}}$. Thus we may begin with a calculation of T_c^{MF} which can serve as an upper bound on the true T_c .

Consider a spin at site i in the pyrochlore lattice. Expanding in small fluctuations about any ground state, we have the same mean-field Hamiltonian as in the general mean field *Ansatz* of section III, with the mean field given by eqn. 4. In a mean-field treatment, each

of the neighbor spins \hat{n}_j is to be replaced by its average $\vec{m}_j = \langle \hat{n}_j \rangle = m\hat{e}_j$ in the particular ground state that we are considering. In any ground state, we note that the angle between any pair of nearest neighbors is $\vartheta_{ij} = \cos^{-1}(-\frac{1}{3})$. In addition, the spins on a tetrahedron add to zero, which allows us to write $\sum_j' \vec{m}_j = -\vec{m}_i$. If we further recall that each spin lies on exactly two tetrahedra, we obtain the following expression for the mean field acting at site i :

$$\vec{h}_i = -\sum_j' \frac{\vec{m}_j}{1 - \vec{m}_i \cdot \vec{m}_j} = \frac{2m}{1 + \frac{m^2}{3}} \hat{e}_i \quad (11)$$

Note that we have only made use of the *local* structure of the ground state, and so our treatment here is relevant for the transition into any state in the ground state manifold. Substituting the mean field in eq. 11 into the self-consistency condition (eqn.6), we find, in a manner similar to the bipartite case, that the mean-field estimate of the transition temperature is $T_c^{\text{MF}} = \frac{2}{3}$. From this alone we conclude that the $M = 1$ state on the pyrochlore lattice is quantum disordered.

There is little question that the actual T_c is much lower than the mean-field estimate and therefore M_c is much higher than $\frac{3}{2}$, allowing many more quantum disordered states. As is familiar from other highly frustrated magnets, where the ground-state manifold encompasses a vastly degenerate set of states the transition will be driven by the ‘order-by-disorder’ mechanism wherein a particular state or subset of states is favored by entropic effects at low temperatures. This is a weak effect and hence T_c is typically a small fraction of T_c^{MF} . From coarse Monte Carlo simulations we find evidence that $T_c < 0.2$ corresponding to $S_c > \frac{1}{2}zM = 15$. This leads already to an AKLT Hamiltonian that is a degree-60 polynomial in the spins and thus there is little reason in the current context to locate the transition or the nature of the ordered phase with greater precision.

However, we note that the same set of ground states arises in the the classical Heisenberg model with nearest neighbor bilinear and biquadratic interactions with the latter chosen to disfavor collinearity. This is a physically plausible model and we will report a fuller investigation of it elsewhere²².

VI. CONCLUDING REMARKS

To summarize, we have studied AKLT states on two unfrustrated and one frustrated lattice in $d = 3$ by a combination of mean-field theory and Monte Carlo simulations for the associated classical models. We find that the simple cubic lattice is Néel ordered at all values of the singlet parameter M and spin S ; the diamond lattice, on the other hand, is quantum-disordered for $M = 1$ ($S = 2$), and Néel ordered for $M > 1$. On the pyrochlore lattice we find that the $M = 1$ ($S = 3$) model is definitely disordered and the boundary between disorder and order very likely lies above $M = 5$.

While quantum-disordered ground states in low (i.e. one and two dimensions) have often been discussed, three dimensions has historically been the province of long range order. Hence our disordered models on the diamond and pyrochlore lattices significantly expand the set of possibilities for quantum ground states of models with Heisenberg symmetry in $d = 3$.

In recent work, one of us has generalized the AKLT construction to $SU(N)$ spins⁹. In the near future, we intend to investigate the $SU(4)$ simplex state on the pyrochlore lattice introduced in this work by methods similar to the ones used in the present paper²³.

Acknowledgments

It is a pleasure to thank Fiona Burnell and Chris Laumann for many discussions and insightful suggestions. David Huse provided invaluable guidance on writing efficient Monte Carlo code. We are also grateful to Roderich Moessner for several conversations about the structure of ground states and the potential for order-by-disorder on the pyrochlore lattice. SAP acknowledges the hospitality of the Institute for Mathematical Sciences, Chennai, India, and the Ecole de Physique des Houches, Les Houches, France, where parts of this work were completed. This work was supported in part by NSF Grant No. DMR 0213706 (SLS).

* Electronic address: sashok@princeton.edu

† Electronic address: sondhi@princeton.edu

‡ Electronic address: darovas@ucsd.edu

¹ I. Affleck, T. Kennedy, E. H. Lieb, and H. Tasaki, *Phys. Rev. Lett.* **59**, 799 (1987); *Comm. Math. Phys* **115**, 477 (1988).

² P. W. Anderson, *Mater. Res. Bull.* **8**, 153 (1973); P. Fazekas and P. W. Anderson, *Phil. Mag.* **30**, 423 (1974).

³ More precisely the ideas of P. W. Anderson, *Science* **235**, 1196 (1987).

⁴ For a review, see S. Sachdev, in *Low dimensional quantum*

field theories for condensed matter physicists, Yu Lu, S. Lundqvist, and G. Morandi eds., World Scientific, Singapore (1995); cond-mat/9303014.

⁵ J.T. Chayes, L. Chayes, and S.A. Kivelson, *Commun. Math. Phys.* **123**, 53 (1989).

⁶ K.S. Raman, R. Moessner, and S.L. Sondhi, *Phys. Rev. B* **72**, 066413 (2005).

⁷ D.J. Klein, *J. Phys. A* **15**, 661 (1982).

⁸ See also the closely related work on an XXZ model in $d = 3$. M. Hermele, M.P.A. Fisher, and L. Balents, *Phys. Rev. B* **69**, 064404 (2004).

- ⁹ D. P. Arovas, *Phys. Rev. B* **77**, 104404 (2008).
- ¹⁰ D. P. Arovas, A. Auerbach, and F. D. M. Haldane, *Phys. Rev. Lett.* **60**, 531 (1988).
- ¹¹ E. J. Neves and J. F. Perez, *Phys. Lett.* **114A**, 331 (1986).
- ¹² This approach was suggested to us by D. Huse; it is also described in Robert G. Brown and Mikael Ciftan, *Phys. Rev. B* **54**, 15860 (1996).
- ¹³ P. Peczak, A.M. Ferrenberg and D.P. Landau, *Phys. Rev. B* **43**, 6087 (1991).
- ¹⁴ System configurations were recorded after each lattice sweep, so 1 MCS is the natural unit of time along the Markov chains. A precise determination of the autocorrelation time was not performed, but plots of the error estimate were made for blocks of increasing length and initial position along the chain, which allowed us to check the convergence of physical quantities; the final block, consisting of the latter half of the chain, was used to perform averages in each thread.
- ¹⁵ K. Binder, *Z. Physik B* **43**, 119 (1981).
- ¹⁶ M.E. Fisher, *Rep. Prog. Phys.* **30**, 615-730 (1967).
- ¹⁷ H.E. Stanley, *Phys. Rev.* **158**, 546 (1967).
- ¹⁸ R. Moessner and J.T. Chalker, *Phys. Rev. Lett.* **80**, 2929 (1998); *Phys. Rev. B* **58**, 12049 (1998).
- ¹⁹ S. V. Isakov, K. Gregor, R. Moessner, and S. L. Sondhi, *Phys. Rev. Lett.* **93**, 167204 (2004).
- ²⁰ D. A. Huse and A.D. Rutenberg, *Phys. Rev. B* **45**, 7536 (1992)
- ²¹ R.J. Baxter, *J. Math. Phys* **11**, 784 (1970.) The problem discussed here is the three-coloring problem on the 2d hexagonal lattice, which is equivalent to the model discussed in Ref. 20.
- ²² S. A. Parameswaran, S.L. Sondhi, D.P. Arovas, R. Moessner, work in progress.
- ²³ S. A. Parameswaran, S.L. Sondhi, D.P. Arovas, work in progress.